

Multiparametric *in vitro* genotoxicity assessment of different variants of amorphous silica nanomaterials in rat alveolar epithelial cells

Fátima Brandão, Carla Costa, Maria João Bessa, Vanessa Valdiglesias, Bryan Hellack, Andrea Haase, Sónia Fraga & João Paulo Teixeira

To cite this article: Fátima Brandão, Carla Costa, Maria João Bessa, Vanessa Valdiglesias, Bryan Hellack, Andrea Haase, Sónia Fraga & João Paulo Teixeira (19 Oct 2023): Multiparametric *in vitro* genotoxicity assessment of different variants of amorphous silica nanomaterials in rat alveolar epithelial cells, *Nanotoxicology*, DOI: [10.1080/17435390.2023.2265481](https://doi.org/10.1080/17435390.2023.2265481)

To link to this article: <https://doi.org/10.1080/17435390.2023.2265481>



© 2023 The Author(s). Published by Informa UK Limited, trading as Taylor & Francis Group



View supplementary material [↗](#)



Published online: 19 Oct 2023.



Submit your article to this journal [↗](#)



Article views: 140



View related articles [↗](#)



View Crossmark data [↗](#)

Multiparametric *in vitro* genotoxicity assessment of different variants of amorphous silica nanomaterials in rat alveolar epithelial cells

Fátima Brandão^{a,b,c,d} , Carla Costa^{a,b,c} , Maria João Bessa^{a,b,c,d} , Vanessa Valdiglesias^{e,f} , Bryan Hellack^{g,h} , Andrea Haaseⁱ , Sónia Fraga^{a,b,c,j}  and João Paulo Teixeira^{a,b,c} 

^aDepartment of Environmental Health, National Institute of Health Dr. Ricardo Jorge, Porto, Portugal; ^bEPIUnit-Institute of Public Health, University of Porto, Porto, Portugal; ^cLaboratory for Integrative and Translational Research in Population Health (ITR), Porto, Portugal; ^dInstitute of Biomedical Sciences Abel Salazar (ICBAS), University of Porto, Porto, Portugal; ^eDepartamento de Biología, Universidad de Coruña, Grupo NanoToxGen, Centro Interdisciplinar de Química e Biología - CICA, A Coruña, Spain; ^fInstituto de Investigación Biomédica de A Coruña (INIBIC), A Coruña, Spain; ^gInstitute of Energy and Environmental Technology (IUTA) e.V, Duisburg, Germany; ^hGerman Environment Agency (UBA), Dessau, Germany; ⁱDepartment of Chemical and Product Safety, German Federal Institute for Risk Assessment (BfR), Berlin, Germany; ^jDepartment of Biomedicine, Unit of Pharmacology and Therapeutics, Faculty of Medicine, University of Porto, Porto, Portugal

ABSTRACT

The hazard posed to human health by inhaled amorphous silica nanomaterials (aSiO₂ NM) remains uncertain. Herein, we assessed the cyto- and genotoxicity of aSiO₂ NM variants covering different sizes (7, 15, and 40 nm) and surface modifications (unmodified, phosphonate-, amino- and trimethylsilyl-modified) on rat alveolar epithelial (RLE-6TN) cells. Cytotoxicity was evaluated at 24 h after exposure to the aSiO₂ NM variants by the lactate dehydrogenase (LDH) release and WST-1 reduction assays, while genotoxicity was assessed using different endpoints: DNA damage (single- and double-strand breaks [SSB and DSB]) by the comet assay for all aSiO₂ NM variants; cell cycle progression and γ -H2AX levels (DSB) by flow cytometry for those variants that presented higher cytotoxic and DNA damaging potential. The variants with higher surface area demonstrated a higher cytotoxic potential (SiO₂_7, SiO₂_15_Unmod, SiO₂_15_Amino, and SiO₂_15_Phospho). SiO₂_40 was the only variant that induced significant DNA damage on RLE-6TN cells. On the other hand, all tested variants (SiO₂_7, SiO₂_15_Unmod, SiO₂_15_Amino, and SiO₂_40) significantly increased total γ -H2AX levels. At high concentrations (28 μ g/cm²), a decrease in G₀/G₁ subpopulation was accompanied by a significant increase in S and G₂/M sub-populations after exposure to all tested materials except for SiO₂_40 which did not affect cell cycle progression. Based on the obtained data, the tested variants can be ranked for its genotoxic DNA damage potential as follows: SiO₂_7 = SiO₂_40 = SiO₂_15_Unmod > SiO₂_15_Amino. Our study supports the usefulness of multiparametric approaches to improve the understanding on NM mechanisms of action and hazard prediction.

ARTICLE HISTORY

Received 1 March 2023
Revised 23 July 2023
Accepted 20 September 2023

KEYWORDS



Silica nanomaterials;
cytotoxicity; genotoxicity;
in vitro; lung


1. Introduction

Nanotechnology is a fast-growing field associated with the development and use of nanomaterials (NM) that exhibit unique and/or improved physico-chemical properties given their nanoscale size and high surface area per unit mass (Shatkin 2008). Owing to their attractive properties, NM have a wide range of applications (Clift, Jenkins, and Doak 2020, Vance et al. 2015) that led to an increase in

their production in the last decades. Consequently, human exposure to these materials has also increased, particularly in occupational settings where inhalation is an important route of exposure (Clift, Jenkins, and Doak 2020, Pietroiusti et al. 2018, Stone et al. 2017, Vance et al. 2015).

Despite several efforts, uncertainties with respect to hazards and risks of NM to human health and the environment remain. In this regard, the

CONTACT Sónia Fraga  sonia.fraga@insa.min  Departamento de Saúde Ambiental, Instituto Nacional de Saúde Doutor Ricardo Jorge, Rua Alexandre Herculano, 321, 4000-055 Porto, Portugal

 Supplemental data for this article can be accessed online at <https://doi.org/10.1080/17435390.2023.2265481>.

© 2023 The Author(s). Published by Informa UK Limited, trading as Taylor & Francis Group
This is an Open Access article distributed under the terms of the Creative Commons Attribution License (<http://creativecommons.org/licenses/by/4.0/>), which permits unrestricted use, distribution, and reproduction in any medium, provided the original work is properly cited. The terms on which this article has been published allow the posting of the Accepted Manuscript in a repository by the author(s) or with their consent.

genotoxicity of NM is an aspect of special concern, since DNA or chromosomal damage may lead to mutations, which in turn can increase the risk of cancer development and/or other diseases (El Yamani et al. 2017, Kryston et al. 2011). Available studies on the genotoxic potential of NM often lack a correlation between *in vivo* and *in vitro* findings, making data inconsistent and contradictory (Chen et al. 2014, Gurcan et al. 2020, Yazdimamaghani et al. 2019). Several aspects make NM toxicity profile evaluation complex, namely the large number of available NM variants, whose intrinsic properties (as synthesized), as well as the method of NM synthesis (e.g. pyrogenic, sol-gel, microemulsion) that have been shown to influence their toxicity profile (Croissant et al. 2020, Karkossa et al. 2019, Tsuji et al. 2006, Zhang et al. 2012). Consequently, their safety assessment has been carried out on a case-by-case basis (Kwon, Koedrith, and Seo 2014). At the same time, NM intrinsic properties might be modified by the environment, which can influence NM interactions and effects on the biological systems (Kroll et al. 2011, Kwon, Koedrith, and Seo 2014). In addition, factors related to the study experimental design including the test systems used that can exhibit different sensitivity, the exposure conditions (e.g. medium composition, dose range, and exposure time), as well as NM ability to interfere with assay components make toxicity data hard to compare (Ajdary et al. 2018, Guadagnini et al. 2015, Kroll et al. 2011, Kroll et al. 2012, Pauluhn 2009).

To overcome these issues, NM safety assessment needs to be done in a comprehensive manner following standardized protocols to reduce experimental variation. Several EU and national projects have meanwhile undertaken huge efforts to better define and harmonize NM genotoxicity testing (summarized in Dusinska et al. (2019)).

So far, the available literature supports the ability of NM to induce genotoxicity through direct interactions of the NM with DNA, however, the genotoxic damage seems to arise mostly from indirect mechanisms, such as NM interactions with other molecules important to DNA replication and repair or from secondary mechanisms as oxidative stress and inflammation (Chen et al. 2014, Gurcan et al. 2020, Swedish Chemicals Agency 2016, Yazdimamaghani et al. 2019). Accordingly, a battery

of assays covering different mechanisms is recommended for assessing NM genotoxicity, though no strict protocol exists. The OECD guidelines for genotoxicity testing, with the exception of the Ames test, seem to be suitable for NM. However, these guidelines have not yet been formally validated for NM, and special attention should be paid to some experimental details (OECD 2014). Thus, for *in vitro* NM genotoxicity testing, a gene mutation test, preferably in mammalian cells, such as the mouse lymphoma assay (MLA) (OECD 2016d) or the hypoxanthine-guanine phosphoribosyl transferase gene (HPRT) test (OECD 2016b), in combination with a chromosome mutation test such as the cytokinesis-block micronucleus (CBMN) test (OECD 2016c) or the chromosomal aberration (CA) test (OECD 2016a) is recommended (Doak and Dusinska 2017, Landsiedel et al. 2022). Regardless, other assays can provide useful information on NM mechanisms of action. The comet assay has been proved to be a simple and sensitive method to assess early DNA damage such as single- and double-strand breaks (SSB and DSB), alkali-labile sites, being one the most used assays for genotoxicity testing of NM (Azqueta and Dusinska 2015, Doak and Dusinska 2017). To maintain genome integrity, cells have developed complex mechanisms of DNA damage response (DDR) that act to repair damage and minimize the odds of lethal or permanent genetic damage. DDR encompasses multiple repair mechanisms and signal transduction pathways, including cell cycle checkpoint arrest and/or apoptosis (Smith et al. 2010). Among the different forms of DNA damage, DSB are the most severe lesions that can lead to chromosome alterations, genomic instability, and even to tumorigenesis if not efficiently repaired (Wan et al. 2019). In response to DSB induction, histone H2AX molecules are rapidly phosphorylated at serine 139 (Ser 139) of DSB sites, referred to as gamma-H2AX (γ -H2AX) foci (Rogakou et al. 1998, Valdiglesias et al. 2013). This early DDR event causes chromatin remodeling and may provide a platform for the recruitment of other enzymes responsible for DSB signaling and DNA repair (Podhorecka, Skladanowski, and Bozko 2010), hence γ H2AX levels are considered a biomarker of DNA repair and genomic instability (Huang and Darzynkiewicz 2006, Nikolova, Marini, and Kaina 2017, Valdiglesias et al. 2013).

Amorphous silica (aSiO₂) NM are extensively used in many fields (Nayl et al. 2022). They can be synthesized by different methods (physical, chemical, biological) in varying sizes and surface functionalities. All these factors (size, surface modification, and synthesis method) can contribute for their toxicological potential though their exact contribution is not yet well understood (Croissant et al. 2020). Herein, we have investigated the *in vitro* cyto- and genotoxic potential of a set of seven aSiO₂ NM variants with different size (7, 15, and 30 nm) and surface modification (unmodified, phosphonate [negatively charged], aminopropyltrimethoxysilane [positively charged] and trimethylsilyl-modified [2 and 3%; different degrees of hydrophobicity]). The rat RLE-6TN cell line was chosen as *in vitro* model for assessing pulmonary toxicity of the NM due to its similarity to alveolar type II epithelial cells and its established usefulness in studying human alveolar cell function (Jiao et al. 2017, Oda et al. 2011). On a first step, all aSiO₂ NM variants were tested for cytotoxicity and DNA damage (comet assay). On a second step, the most toxic aSiO₂ NM variants were selected to further explore the mechanisms involved in genotoxicity and/or associated DNA repair responses. For that purpose, we assessed cell cycle progression and γ -H2AX content by flow cytometry in alveolar epithelial cells exposed to the most toxic aSiO₂ NM variants.

2. Materials and methods

2.1. Chemicals and reagents

All chemicals used were of high purity or analytical grade. Bovine serum albumin (BSA; CAS No. 9048-46-8), Triton X-100 (CAS No. 9002-93-1), propidium iodide (PI; CAS No. 25535-16-4), insulin from bovine pancreas (11070-73-8), insulin-like growth factor (IGF; CAS No. 67763-96-6), epidermal growth factor (EGF; CAS No. 62253-63-8), human apo-transferrin (CAS No. 11096-37-0), Accutase[®] solution, low melting point agarose (LMP; CAS No. 39346-81-1), Tris hydrochloride (Tris-HCl; CAS No. 1185-53-1), methyl methanesulfonate (MMS; CAS No. 66-27-3), dimethyl sulfoxide (DMSO; CAS No. 67-68-5), Pluronic[®] F-108 (CAS No. 9003-11-6), camptothecin (CPT; CAS No. 7689-03-4), ribonuclease A from bovine pancreas (RNAse A; CAS No. 9001-99-4), Roche cytotoxicity

detection kit (LDH), and cell proliferation reagent water-soluble tetrazolium (WST-1) were purchased from Sigma-Aldrich (Madrid, Spain). Sodium hydroxide (NaOH; CAS No. 1310-73-2), sodium chloride (NaCl; CAS No. 7647-14-5), potassium chloride (KCl; CAS No. 7447-40-7), potassium hydroxide (KOH, CAS No. 1310-58-3) were bought from Merck KGaA (Darmstadt, Germany). Tris-base (CAS No. 77-86-1) and disodium salt dihydrate (Na₂EDTA; CAS No. 6381-92-6) were purchased from Merck Millipore (Madrid, Spain). Phosphate buffered saline (PBS) was purchased from Lonza (Lutterworth, UK). Normal melting point (NMP) agarose (CAS No. 9012-36-6) was supplied by Biotline (London, UK). Invitrogen[™] SYBR[®] Gold, L-glutamine solution (Gibco; CAS No. 56-85-9), bovine pituitary extract (Gibco), Ham's F-12 medium with 1 mM L-glutamine (Gibco), eBioscience[™] phospho-histone H2A.X (Ser139) Alexa Fluor[®] 488 conjugated monoclonal antibody (CR55T33) and Recovery[™] freezing medium (Gibco) were purchased from Thermo Fisher Scientific (Madrid, Spain). Penicillin-streptomycin solution (10,000 U/mL penicillin and 10 mg/mL streptomycin) and fetal bovine serum (FBS) were supplied by PANTM Biotech (Aidenbach, Germany). Bleomycin sulfate (BLM; CAS No. 9041-93-4) was purchased from Cayman Chemical (Ann Harbor, USA).

2.2. Nanomaterials (NM) dispersion and characterization

In this study, a set of seven aSiO₂ NM variants, differing in size (7, 15, and 40 nm) and surface modification (unmodified, trimethylsilyl [2 and 3%], aminopropyltrimethoxysilane and phosphonate) were tested: SiO₂_7, SiO₂_7_TMS2, SiO₂_7_TMS3, and SiO₂_40 provided by Evonik Industries Resource Efficiency GmbH (Hanau, Germany); SiO₂_15_Unmod, SiO₂_15_Amino, and SiO₂_15_Phospho provided by BASF SE (Mannheim, Germany). All tested aSiO₂ NM variants were sterilized by gamma-irradiation and confirmed to be endotoxin-free by the Limulus amoebocyte lysate (LAL) test, as previously reported (Bahl et al. 2019, Karkossa et al. 2019). Stock suspensions of all NM (0.5 mg/mL) were freshly prepared and diluted in serum-free cell culture medium immediately before use. Hydrophilic NM (SiO₂_7, SiO₂_15_Unmod, SiO₂_15_Amino, SiO₂_15_Phospho, SiO₂_40) were dispersed by indirect

probe sonication using a Bandelin cup horn (Berlin, Germany) according to an internal Standard Operating Procedure (SOP) developed within NanoToxClass (NanoToxClass 2017). For dispersion of the hydrophobic NM (SiO₂_7_TMS2 and SiO₂_7_TMS3), 100 µg/mL of Pluronic[®] F-108 was added as dispersant agent prior sonication. The tested NM were extensively characterized both in deionized water (dH₂O) and in serum-free cell culture medium using state-of-the-art techniques (Bahl et al. 2019, Karkossa et al. 2019). Table S1 presents some of the main physicochemical properties of the NM, namely hydrodynamic diameter, zeta potential, redox potential, and dissolution rate. All tested aSiO₂ NM exhibited spherical shape as assessed by Scanning Electron Microscopy (SEM), as depicted in Table S2.

2.3. Cell culture

Rat alveolar type II epithelial RLE-6TN cells (passage 39) were obtained from the American Type Culture Collection (ATCC; CRL-2300TM; Manassas, USA). Cells were cultured in Ham's F12 medium supplemented with 2 mM L-glutamine, 0.01 mg/mL bovine pituitary extract, 0.005 mg/mL insulin, 2.5 ng/mL IGF, 0.00125 mg/mL apo-transferrin, and 2.5 ng/mL EGF, 10% heat-inactivated FBS, 100 U/mL penicillin, and 100 µg/mL streptomycin, and grown at 37 °C, 5% CO₂ in a humidified atmosphere. Cells of an early passage were subcultured twice a week at a 1:2 split ratio, using Accutase[®] solution to a maximum of 20 passages. For toxicity assessment, cells (circa 80% confluence) were detached and seeded in 96- or 12 well-plates, depending on the assay. The cell media was changed 24 h after seeding and the cells were allowed to grow for further 24 h until exposure.

2.4. Assessment of the cytotoxic effects induced by the aSiO₂ NM variants

Cells were seeded in 96-well plates (2×10^4 cells/well) and incubated with increasing concentrations (0–56 µg/cm²; 200 µL) of the tested NM, serum-free cell medium (NC), and vehicle (serum-free cell culture media containing 100 µg/mL of Pluronic[®] F-108 as dispersant) during 24 h at 37 °C, 5% CO₂. Two cytotoxicity endpoints were determined: lactate dehydrogenase (LDH) release and WST-1

reduction, indicators of plasma membrane integrity and metabolic (mitochondrial) activity, respectively. LDH release was determined using the Cytotoxicity Detection Kit (Roche, Mannheim, Germany), according to manufacturer's instructions. Following the exposure period, incubation media were gently pipetted to a 96-well round bottom microplate and centrifuged for 5 min at 2210 × g to remove the cell debris and residual NM. Cells lysed with 0.2% Triton X-100 (30 min) for total LDH release were used as the positive control (PC). Briefly, 100 µL of freshly prepared reaction mixture was added to 100 µL of each sample and incubated at room temperature (RT), protected from light. Absorbance was measured at 490 and 655 nm (reference wavelength) in a Cambrex ELx808 microplate reader (Biotek, Winooski, USA). LDH release values were normalized considering the total LDH release (PC) using the following equation: $(\text{optical density [OD] sample} - \text{OD blank}) / (\text{mean OD PC} \times 100)$, where the blank corresponds to cell medium containing the same concentration of the respective aSiO₂ NM variant. To test for possible NM interferences, total LDH release was determined in the absence and in the presence of the highest tested concentration of each aSiO₂ NM variant. Cell metabolic activity was evaluated using WST-1 Cell Proliferation Reagent Kit (Roche, Mannheim, Germany), according to the manufacturer's instructions. Cells exposed to ethanol 70% (30 min) were used as PC. After exposure, the incubation medium was removed and cells washed with PBS pH 7.4 prior incubation for 2 h at 37 °C, 5% CO₂ with 100 µL/well of WST-1 reagent diluted 1:10 in serum-free cell culture medium. Sample's absorbance was measured at 450 and 630 nm (reference wavelength) in a Cambrex ELx808 microplate reader. To test for potential interferences of the aSiO₂ NM in the assay, PC was determined in the absence and in the presence of the highest tested concentration of each aSiO₂ NM variant. WST-1 reduction values were normalized considering the NC mean value according to the following formula $(\text{OD sample}) / (\text{mean NC} \times 100)$. Moreover, for both assays a cell-free system test with the NM-tested concentrations was conducted in order to evaluate a potential activation of the assay enzymatic reactions by NM.

2.5. Assessment of the genotoxic effects induced by the aSiO₂ NM

The genotoxic potential and DDR were investigated by evaluating DNA damage, phosphorylation of histone H2AX (γ -H2AX) and changes in the cell cycle of RLE-6TN cells after 24 h of exposure to the aSiO₂ NM.

2.5.1. DNA damage

DNA damage was assessed by the alkaline comet assay as previously described by Bessa et al. (2017), with slight modifications. Minimum Information for Reporting Comet Assay procedures and results (MIRCA) recommendations were followed in this manuscript (Moller et al. 2020). Briefly, RLE-6TN cells were seeded into 12-well plate (5×10^5 cells/well) and incubated for 24 h at 37 °C, 5% CO₂ in a humidified atmosphere with non-cytotoxic concentrations of the NM (7–28 $\mu\text{g}/\text{cm}^2$) and the alkylating agent MMS (250 μM) used as PC. After NM incubation, cells were rinsed 3 times with PBS pH 7.4 (w/o Ca and Mg) and gently harvested using a scraper. The cell suspensions were transferred to a microcentrifuge tube and centrifuged for 5 min at $500 \times g$. The supernatant removed, the pellet gently resuspended in 200 μL of PBS 7.4 and kept on ice. Cell density was determined using a Neubauer cell chamber and 8×10^3 cells/200 μL in PBS pH 7.4 were transferred to a microtube and centrifuged for 5 min at $700 \times g$. Subsequently, the supernatants were discarded, and cells embedded in 100 μL of 1% LMP agarose. Then, 5 μL of each sample (400 cells per gel) were loaded in duplicate onto dry microscope slides precoated with 1% NMP using a medium throughput 12-gel comet assay unit (Severn Biotech Ltd.[®], Kidderminster, UK). Slides were maintained for 5 min at 4 °C for gel polymerization and after that immersed in ice-cold lysis solution (2.5 M NaCl, 100 mM Na₂EDTA, 10 mM Tris-base, 10 M NaOH pH 10, 1% Triton-X 100) during 1 h at 4 °C, protected from light. After lysis, slides were washed 3 times with PBS 7.4 for 5 min and immersed in electrophoresis solution (1 mM Na₂EDTA, 0.3 M NaOH pH 13) in the electrophoresis platform for DNA unwinding for 40 min, followed by electrophoresis in the same solution for 30 min at constant 25 V (0.9 V/cm) and 400 mA. The slides were then washed with ice-cold PBS pH 7.4 and

ice-cold dH₂O for 10 min each, followed by fixation with ethanol (70%) and ethanol (96%) for 15 min each, and the slides dried overnight. Prior to scoring, slides were stained with a 1:10,000 dilution of SYBR[®] Gold in Tris-EDTA buffer (10 mM Tris-HCl, 1 mM EDTA, pH 7.5–8). The slides were scored using a fluorescence microscope (Motic BA410 ELITE) attached to an epifluorescence illuminator (Filter Set: Exciter D480/30x, Emitter D535/40 nm, Dichroic 505DCLP) with a 100 \times magnification, using the image analysis software Comet Assay IV (Perceptive Instruments, Suffolk, UK). Three independent experiments with two biological replicates/experiment were performed. At least 100 cells/replicate (50 in each replicate gel) were analyzed in each replicate slide. Percentage of DNA in the comet tail (% DNA in tail) was used as DNA damage descriptor.

2.5.2. Cell cycle progression and histone H2AX phosphorylation (γ -H2AX) analysis

Potential changes in the cell cycle, as well as phosphorylation of histone gamma-H2AX (γ -H2AX) at Ser 139 residue were assessed in parallel in the same samples by flow cytometry, as previously described by Valdiglesias et al. (2011) for the γ -H2AX histone and by Rosário et al. (2020) for the cell cycle, with minor modifications. Briefly, RLE-6TN cells were seeded into 12-well plates (2×10^5 cells/well) and incubated for 24 h with sub-cytotoxic concentrations (7–28 $\mu\text{g}/\text{cm}^2$) of the aSiO₂ NM (SiO₂_7, SiO₂_15_Unmod, SiO₂_15_Amino, and SiO₂_40). Briefly, after the exposure period, the incubation medium was aspirated, and the cells rinsed three times with 500 μL of PBS 7.4. Then, cells were gently harvested by incubation with 250 μL of Accutase[®] solution for 5 min at 37 °C and inactivated with 500 μL of complete cell culture medium. The cell suspensions were transferred to centrifuge tubes, centrifuged for 5 min at $200 \times g$ and the supernatants discarded. The pellets were suspended in 1 mL of pre-chilled ethanol 70% for fixation and membrane permeabilization and stored at –20 °C until further analysis. At the time of analysis, cells were centrifuged at $300 \times g$ for 5 min, the supernatants were removed, and the pellets suspended in 1 mL of flow cytometry grade PBS (PBScit) supplemented with 1% BSA. Then, cell suspensions were centrifuged again for 5 min at $300 \times g$, the supernatants discarded, and cells were labeled with 100 μL

of 5 $\mu\text{g}/\text{mL}$ phospho-histone H2AX (Ser139) Alexa Fluor[®] 488 conjugated monoclonal antibody for 15 min at RT, protected from light. Thereafter, 1 mL of 1% BSA in PBScit was added to each sample, followed by sample centrifugation for 5 min at $300 \times g$. The supernatants were discarded, and the pellets suspended in staining solution (50 $\mu\text{g}/\text{mL}$ of PI, 50 $\mu\text{g}/\text{mL}$ of RNase A prepared in ultrapure water) for 30 min at RT, protected from light. Samples were then filtered through a 70 μm cell strainer to remove residual NM and reduce cell clumping. Acquisitions were made using Guava[®] easyCyte[™] flow cytometer (Merck KGaA, Darmstadt, Germany). For each sample, 1×10^4 events were recorded at a low flow rate (0.24 $\mu\text{L}/\text{s}$). Debris and doublets were excluded by plotting width against area for side scatter (SSC). For γ -H2AX analysis, gating was based on dot plot (Red-B height linear scale vs. Green-B height log scale) with quadrants, defined based on the PC samples (i.e. cells exposed to 10 $\mu\text{g}/\text{mL}$ of BLM for 4 h). For cell cycle analysis, % of nuclei in each phase of the cell cycle (G_0/G_1 , S and G_2/M -phases) was based on the histogram outputs for Red-B peak height linear scale. The expression of γ -H2AX in each phase of the cell cycle was also determined using the dot plot (Red-B height linear scale vs. Green-B height log scale) gated for each cell cycle phase. The % sub G_1 population was also calculated and used as an indicator of apoptosis. Figure S1 presents histograms obtained for NC and variants of SiO_2 NM in cell cycle analysis, and the corresponding dot plots used for γ -H2AX analysis.

2.6. Statistical analysis

All data were expressed as mean \pm standard deviation (SD) of three independent experiments. Statistical analyses of data were performed using GraphPad Prism version 6 for Windows (La Jolla, USA). Data were tested for normal distribution and homogeneity of variances by D'Agostino-Pearson omnibus and Levene's tests, respectively. Cytotoxicity, γ -H2AX, and cell cycle data were analyzed by one-way ANOVA followed by Dunnett's test for multiple comparisons. Comet assay data were analyzed by the Kruskal-Wallis test followed by the Dunn's multiple comparisons test. Concentration-response curves were obtained using

the method of least squares and half-maximal and 25% inhibitory concentrations (IC_{50} and IC_{25}) values were calculated. Significance was considered at a p value < 0.05 .

3. Results

3.1. In vitro cytotoxicity assessment

In vitro cytotoxicity testing of the selected a SiO_2 NM variants was carried out to select of sub-cytotoxic concentrations for *in vitro* genotoxicity testing, thereby ensuring reliability of data. Overall, both cytotoxicity assays demonstrated to be suitable for assessing the cytotoxic potential of the selected panel of NM under study. As depicted in Figure 1, under serum-free conditions, SiO_2 _7, SiO_2 _15_Unmod, SiO_2 _15_Amino, and SiO_2 _15_Phospho were the most cytotoxic among the a SiO_2 NM variants tested, while exposure to the trimethylsilyl-modified hydrophobic a SiO_2 NM, either SiO_2 _7_TMS2, or SiO_2 _7_TMS3, did not induce significant cytotoxicity on RLE-6TN cells. SiO_2 _7 markedly decreased both cellular metabolic activity and plasma membrane integrity. Amino- and phosphonate surface modification significantly decreased SiO_2 _15 cytotoxicity as evidenced by the higher half-maximal inhibitory concentration (IC_{50}) values obtained from WST-1 concentration-response curves, 55.1 and 59.3 $\mu\text{g}/\text{cm}^2$, respectively, compared to SiO_2 _15_Unmod (34.56 $\mu\text{g}/\text{cm}^2$) (Table 1). Although significant changes in plasma membrane integrity of cells exposed to high concentrations of SiO_2 _40 have been detected, no significant alterations in the metabolic activity were observed. NM interferences did not seem to have occurred since no significant differences in the PC values in the absence vs. in the presence of the highest tested concentration of any tested NM were detected in both assays (data not shown).

3.2. DNA damage

The genotoxic potential of the a SiO_2 NM variants was evaluated by assessing their ability to induce DNA damage in the rat alveolar epithelial (RLE-6TN) cell line. For that purpose, cells were exposed for 24 h to sub-cytotoxic concentrations (0–28 $\mu\text{g}/\text{cm}^2$) of the seven a SiO_2 NM variants and DNA damage was assessed by the alkaline comet assay that detects SSB, DSB, and alkali-labile sites in individual cells (Azqueta and Collins 2013). As shown in Figure 2,

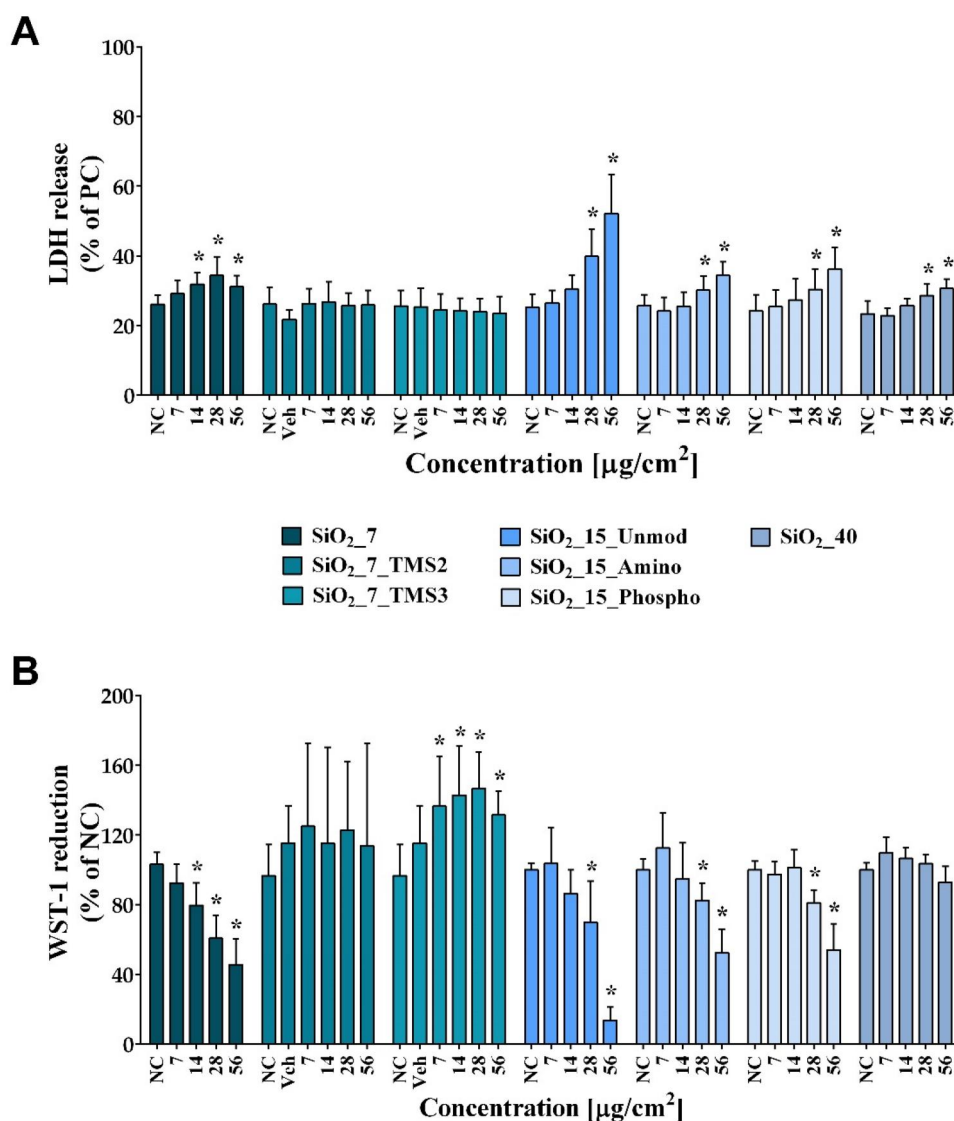


Figure 1. Cytotoxicity of the seven aSiO₂ variants under study in rat alveolar epithelial RLE-6TN cells after 24 h of exposure, measured by lactate dehydrogenase (LDH) release (A) and WST-1 reduction (B). Data are expressed as mean \pm standard deviation of three independent experiments, each performed in triplicate. LDH release values were normalized considering the positive control (PC; cells lysed with 0.2% Triton X-100), while WST-1 reduction values were normalized considering the negative control (NC; serum-free cell culture medium). Vehicle (Veh; serum-free cell culture media containing 100 $\mu\text{g}/\text{mL}$ of Pluronic[®] F-108 as dispersant). Data were analyzed by one-way ANOVA followed by Dunnett's post hoc test for multiple comparisons. * $p < 0.05$ vs. NC.

Table 1. Half-maximal (IC₅₀) and 25% (IC₂₅) inhibitory concentrations for the tested aSiO₂ variants calculated based on data from WST-1 reduction assay concentration-response curves of WST-1 reduction in RLE-6TN after 24 h of exposure.

	WST-1	WST-1
	IC ₅₀	IC ₂₅
	mean (95% CI)	mean (95% CI)
	($\mu\text{g}/\text{cm}^2$)	($\mu\text{g}/\text{cm}^2$)
NM		
SiO ₂ _7	42.6 (32.6 – 55.5)	15.2 (10.2 – 21.7)
SiO ₂ _7_TMS2	NR	NR
SiO ₂ _7_TMS3	NR	NR
SiO ₂ _15_Unmod	34.6 (31.5 – 38.1)	25.3 (22.2 – 28.9)
SiO ₂ _15_Amino	55.1 (45.8 – 66.3)	30.8 (23.0 – 41.1)
SiO ₂ _15_Phospho	59.3 (52.9 – 66.6)	35.2 (29.7 – 41.7)
SiO ₂ _40	NR	NR

NR: not reached

negative control (NC) cells exhibited a very low level of DNA damage close to 5% of DNA in tail. On the other hand, cells exposed to the PC, the alkylating agent MMS (250 μM), were significantly damaged, as expected, with a mean % DNA in tail value of 37.9%. SiO₂_7, either unmodified or trimethylsilyl-modified did not cause any increase in DNA damage levels comparing with NC cells. Similar findings were obtained for SiO₂_15, irrespective of its surface modification. Only SiO₂_40 caused a significant increase in the DNA damage comparing with NC cells, with % DNA in tail values of 11.0 ± 3.8 in cells exposed to

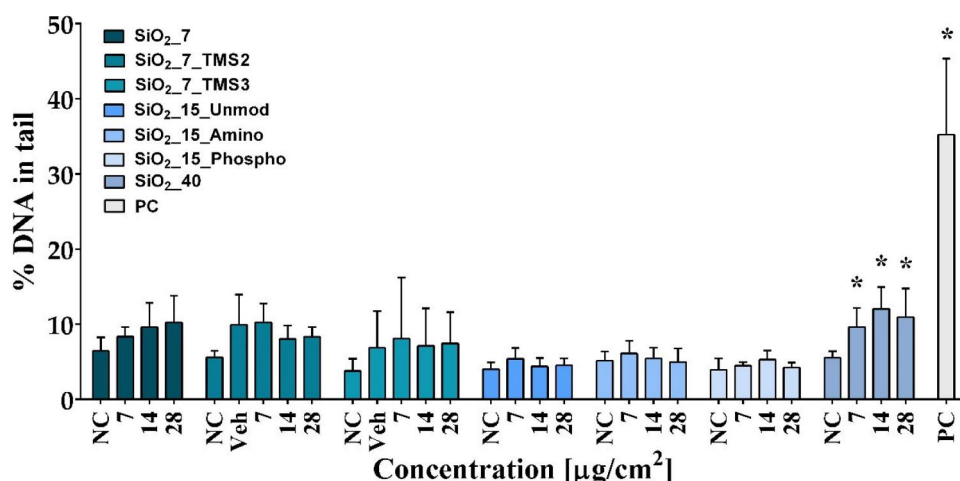


Figure 2. DNA damage (% DNA in tail) of RLE-6TN cells exposed to the aSiO₂ NM variants for 24 h, as assessed using the alkaline comet assay. Negative control (NC; serum-free cell culture medium); Vehicle: (Veh; serum-free cell culture media containing 100 µg/mL of Pluronic® F-108 as dispersant; positive control (PC; cells exposed to 250 µM of methyl methane sulfonate [MMS]). Data are expressed as mean ± standard deviation of three independent experiments, each performed in duplicate. Data were analyzed by Kruskal–Wallis test followed by Dunn’s multiple comparisons. **p* < 0.05 vs. NC.

Table 2. Hazard ranking of the aSiO₂ NM variants based on *in vitro* cyto- and genotoxicity (DNA damage) data sets of rat alveolar epithelial RLE-6TN cells.

NM	Cellular metabolic activity (WST-1 assay)	Cytotoxicity potential	DNA damage (Comet assay)	DNA damage potential
SiO ₂ _7	IC ₅₀ [32.6–55.5] µg/cm ²	High	No changes up to 28 µg/cm ²	Negative
SiO ₂ _7_TMS2	Neither IC ₅₀ nor IC ₂₅ reached up to 56 µg/cm ²	No	No changes up to 28 µg/cm ²	Negative
SiO ₂ _7_TMS3	Neither IC ₅₀ nor IC ₂₅ reached up to 56 µg/cm ²	No	No changes up to 28 µg/cm ²	Negative
SiO ₂ _15_Unmod	IC ₅₀ [31.5–38.1] µg/cm ²	High	No changes up to 28 µg/cm ²	Negative
SiO ₂ _15_Amino	IC ₅₀ [45.8–66.3] µg/cm ²	High	No changes up to 28 µg/cm ²	Negative
SiO ₂ _15_Phospho	IC ₅₀ [52.8–66.6] µg/cm ²	High	No changes up to 28 µg/cm ²	Negative
SiO ₂ _40	Neither IC ₅₀ nor IC ₂₅ reached up to 56 µg/cm ²	No	Significant effect at all tested concentrations; concentration-independent effect	Equivocal

IC₅₀: Half-maximal inhibitory concentration; IC₂₅: 25% inhibitory concentration.

the highest tested concentration. To test for potential interferences of the NM in the comet assay, NC cells were mixed with each NM at the highest tested concentration (28 µg/cm²), combined with LMA (final concentration 1%) and then subjected to the comet assay procedures. For all tested NM, no significant differences in % DNA in tail values compared to the NC were observed, supporting that these NM did not interfere in this analysis (data not shown).

3.3. Hazard ranking

According to the magnitude of the cytotoxic and genotoxic (DNA damage) effects observed in RLE-6TN cells, aSiO₂ NM variants were ranked for hazard based on the criteria listed in Table S3. The

cytotoxicity ranking was based on WST-1 data (IC₅₀/IC₂₅ estimates). Hence, SiO₂_7, SiO₂_15_Unmod, SiO₂_15_Amino, and SiO₂_15_Phospho were ranked as highly cytotoxic (Table 2). In turn, SiO₂_7_TMS2, SiO₂_7_TMS3, SiO₂_40 were classified as non-cytotoxic. Regarding their genotoxic potential, while most of the aSiO₂ NM variants did not cause any change in DNA integrity, being classified as negative, the SiO₂_40 variant induced a significant DNA damage, though not concentration-dependent, being considered as equivocal.

3.4. DNA damage response (DDR)

In order to further explore aSiO₂ NM DNA damage potential and the putative DDR pathways in RLE-

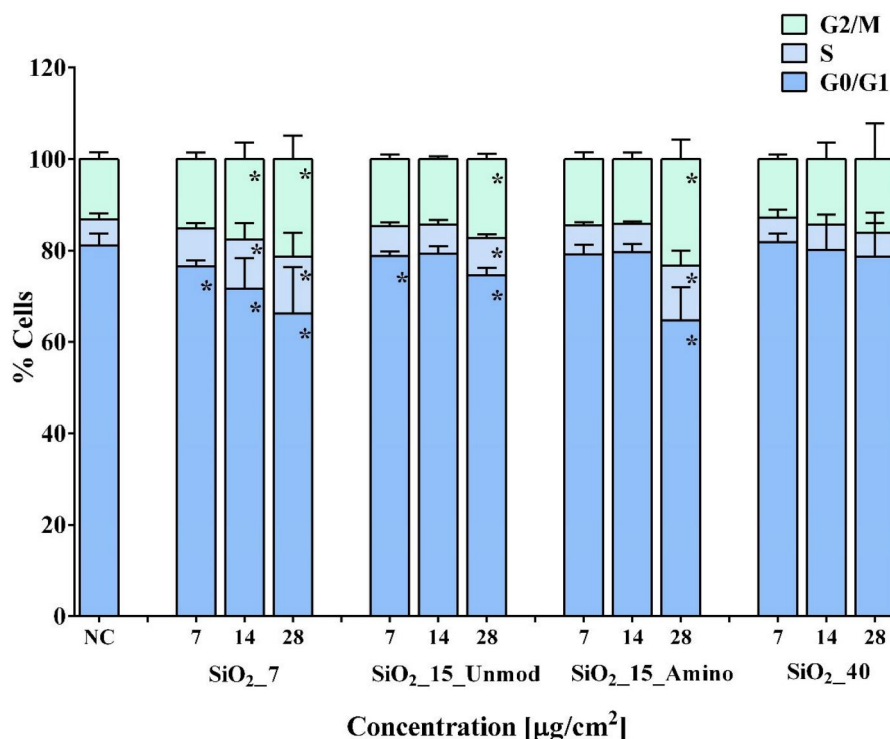


Figure 3. Cell cycle distribution of RLE-6TN cells. Percentage of cells in different phases after exposure for 24h to the four aSiO₂ NM variants tested (SiO₂_7, SiO₂_15_Unmod; SiO₂_15_Amino, and SiO₂_40). Values are expressed as mean ± standard deviation of three independent experiments, each performed in triplicate. Data were analyzed by one-way ANOVA followed by Dunnett's post hoc test. **p* < 0.05 vs. negative control (NC).

6TN cells, we have analyzed cell cycle progression and γ -H2AX content in cells incubated for 24 h with sub-cytotoxic concentrations (0–28 $\mu\text{g}/\text{cm}^2$) of the aSiO₂ NM variants ranked with higher toxic potential (SiO₂_7, SiO₂_15_Unmod, SiO₂_15_Amino, and SiO₂_40) based on cytotoxicity and DNA damage data (Table 2). Under our experimental conditions, i.e. in serum-free incubation medium, G₀/G₁ phase (81.1 ± 2.8%) was the dominant subpopulation compared to S (5.8 ± 1.3%) and G₂/M (13.1 ± 1.5%) phases in NC cells (Figure 3; representative histogram in Figure S1). While exposure to SiO₂_40 did not affect cell cycle progression, some changes in cell cycle subpopulations have been observed after 24 h of exposure to SiO₂_7, SiO₂_15_Unmod, and SiO₂_15_Amino. Exposure to 7, 14 and 28 $\mu\text{g}/\text{cm}^2$ of SiO₂_7 induced a significant decrease in G₀/G₁ subpopulation to 76.5%, 71.7%, and 63.4%, respectively. Moreover, in cells exposed to 14 and 28 $\mu\text{g}/\text{cm}^2$ of SiO₂_7, the decrease in G₀/G₁ subpopulation was accompanied by a significant increase in S and G₂/M subpopulations (14 $\mu\text{g}/\text{cm}^2$: 10.7% in S and 17.6% G₂/M phases; 28 $\mu\text{g}/\text{cm}^2$: 13.8% in S and 22.8% G₂/M phases). A similar trend has been observed in RLE-

6TN cells exposed to SiO₂_15_Unmod that at lower concentrations (7 $\mu\text{g}/\text{cm}^2$) caused a slight but significant reduction in G₀/G₁ cell subpopulation (78.8%) without significantly affecting the other two phases; and at highest tested concentration, SiO₂_15_Unmod led to a significant decrease in G₀/G₁ (74.6%) cell subpopulation at the expense of S (8.2%) and G₂/M (17.2%) phases (Figure 3). In turn, exposure to SiO₂_15_Amino led to a significant decrease in G₀/G₁ subpopulation (64.7%) at the expense of the other two phases (12.0% in S and 23.3% G₂/M phases) only at the highest tested concentration. Considering the number of apoptotic cells, assessed by the sub-G1 cell population, a significant increase was observed after exposure to the highest tested concentration (28 $\mu\text{g}/\text{cm}^2$) of all aSiO₂ NM variant tested (Figure S2), except for SiO₂_40, where a significant increase in the number of apoptotic cells was detected after exposure to 14 $\mu\text{g}/\text{cm}^2$.

Regarding the total γ -H2AX levels, as shown in Figure 4, RLE-6TN cells exhibited a low basal level of γ -H2AX (1.8 ± 0.4%), with 0.9 ± 0.2%, 0.3 ± 0.1%, and 0.6 ± 0.2% of cells in the G₀/G₁, S and G₂/M phases, respectively. As expected, cells exposed to

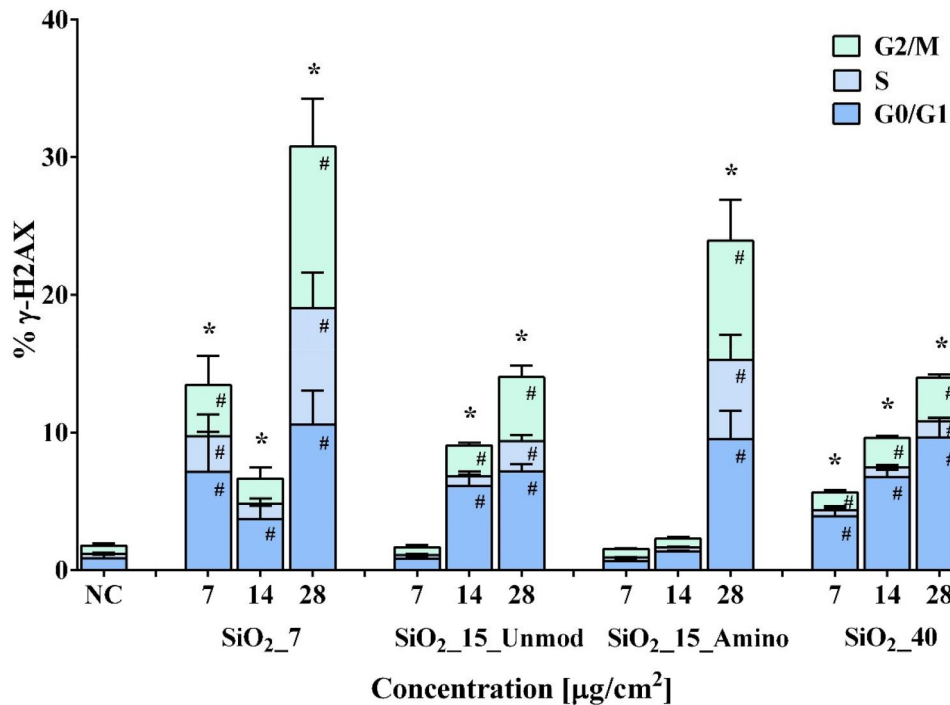


Figure 4. Flow cytometry analysis of histone H2AX phosphorylation in RLE-6TN cells. Percentage of phosphorylated histone H2AX (% γ -H2AX), total and in each cell cycle phase, after exposure to the aSiO₂ NM variants (SiO₂_7, SiO₂_15_Unmod; SiO₂_15_Amino and SiO₂_40). Data are expressed as mean \pm standard deviation of three independent experiments, each performed in duplicate. Data were analyzed by one-way ANOVA followed by Dunnett's post hoc test. Total γ -H2AX: * p < 0.05 vs. NC; γ -H2AX in each phase of cell cycle: # p < 0.05 vs. NC.

bleomycin sulfate (BLM; PC) exhibited a marked increase of total γ -H2AX ($88.6 \pm 3.6\%$), mostly in non-S-phase populations (data not shown), which is in accordance with previous studies (Scarpato et al. 2013, Tomilin et al. 2001). Exposure to any of the tested aSiO₂ NM variants affected γ -H2AX levels of RLE cells. Incubation with SiO₂_7 or SiO₂_40 caused a significant increase in total γ -H2AX levels in cells exposed to all tested concentrations, with SiO₂_7 inducing the highest increase in γ -H2AX ($30.8 \pm 8.2\%$, for the highest tested concentration) compared to NC. In addition, a significant increase of γ -H2AX levels was also detected in cells exposed to the two highest tested concentrations of SiO₂_15_Unmod ($14.0 \pm 0.9\%$, for the highest tested concentration) and in cells exposed to the highest tested of SiO₂_15_Amino ($24.0 \pm 6.8\%$) in relation to the NC. Moreover, at the highest tested concentration ($28 \mu\text{g}/\text{cm}^2$) of any tested variant, the rise in γ -H2AX levels was visible in all phases of the cell cycle, while in cells exposed to other concentrations the increase in γ -H2AX levels was only detected in G₀/G₁ and G₂/M subpopulations,

except for SiO₂_7, where exposure to $14 \mu\text{g}/\text{cm}^2$ only induced an increase of γ -H2AX levels in cells at G₀/G₁ phase but cells incubated with $7 \mu\text{g}/\text{cm}^2$ also showed a significant increase of γ -H2AX in all cell cycle phases (Figure 4).

3.5. Hazard ranking

As shown in Table 3 and according to the criteria depicted in Table S3, SiO₂_7, SiO₂_15_Unmod, and SiO₂_40 were classified as positive, equivocal and negative, for one of the three genotoxicity endpoints assessed. While SiO₂_7 and SiO₂_15_Unmod were both negative for DNA damage as assessed by the comet assay, the former were positive for cell cycle progression and equivocal for γ -H2AX, while the latter were positive for γ -H2AX and equivocal for cell cycle progression. Interestingly, amino surface modification of SiO₂_15 seems to attenuate its genotoxicity potential since SiO₂_15_Amino was assigned as negative for DNA damage and equivocal for both cell cycle progression and total γ -H2AX. On the other hand, SiO₂_40 were positive for γ -H2AX but

Table 3. Hazard ranking of the tested aSiO₂ NM based on the genotoxicity endpoints data sets of rat alveolar epithelial RLE-6TN cells.

NM	DNA damage (Comet assay)	Hazard potential	Cell cycle progression (Flow cytometry)	Hazard potential	Total γ -H2AX (Flow cytometry)	Hazard potential
SiO ₂ _7	No changes up to 28 $\mu\text{g}/\text{cm}^2$	Negative	Changes at all tested concentrations (7–28 $\mu\text{g}/\text{cm}^2$); concentration-dependent trend	Positive	Changes at all tested concentrations (7–28 $\mu\text{g}/\text{cm}^2$); no concentration-dependent trend	Equivocal
SiO ₂ _15_Unmod	No changes up to 28 $\mu\text{g}/\text{cm}^2$	Negative	Changes at 7 and 28 $\mu\text{g}/\text{cm}^2$; no concentration dependent trend	Equivocal	Changes at 14 and 28 $\mu\text{g}/\text{cm}^2$; concentration-dependent trend	Positive
SiO ₂ _15_Amino	No changes up to 28 $\mu\text{g}/\text{cm}^2$	Negative	Changes only at 28 $\mu\text{g}/\text{cm}^2$	Equivocal	Changes only at 28 $\mu\text{g}/\text{cm}^2$	Equivocal
SiO ₂ _40	Changes at all tested concentrations (7–28 $\mu\text{g}/\text{cm}^2$); no concentration-dependent trend	Equivocal	No changes up to 28 $\mu\text{g}/\text{cm}^2$	Negative	Changes at all tested concentrations (7–28 $\mu\text{g}/\text{cm}^2$); concentration dependent trend	Positive

assigned as equivocal for its DNA damaging potential and negative for cell cycle progression. Therefore, considering all genotoxicity endpoints data sets, aSiO₂ NM can be ranked for its hazard to rat alveolar epithelial cells as follows: SiO₂_7 = SiO₂_15_Unmod = SiO₂_40 > SiO₂_15_Amino.

4. Discussion

Alveolar epithelial cells play a major role in lung physiology and are expected targets for inhaled NM (Hiemstra et al. 2018). Hence, we have carried out genotoxicity testing of different aSiO₂ NM variants in the rat alveolar epithelial cell line RLE-6TN using a multiparametric approach. Our data showed that SiO₂_7, SiO₂_15_Unmod, SiO₂_15_Amino, and SiO₂_15_Phospho impacted both membrane integrity and metabolic activity of RLE-6TN cells, being these effects more pronounced in the cells exposed to SiO₂_7 and SiO₂_15_Unmod. In turn, the surface-modified variants SiO₂_7_TMS2, SiO₂_7_TMS3, SiO₂_15_Amino, and SiO₂_15_Phospho demonstrated a lower or no cytotoxic potential, suggesting that surface modification can prevent/mitigate the cytotoxic effects induced by their pristine counterparts. In fact, previous studies demonstrated that surface modification is an effective strategy to prevent the cytotoxic effects of aSiO₂ NM (Großgarten et al. 2018, Kasper et al. 2015, Lankoff et al. 2013, Marzaioli et al. 2014, Yoshida et al. 2012). In this regard, Karkossa et al. (2019) showed significant alterations in the global proteomics, targeted metabolomics and SH2 profiling of RLE-6TN

exposed to SiO₂_7 but not to SiO₂_7_TMS2 and SiO₂_7_TMS3. The hydrophobicity of the organosilane surface-modified variants seems to diminish their bioactivity, given their increased tendency to agglomerate that may impair their uptake, and consequently their toxicity (Halamoda-Kenzaoui et al. 2015, Wiemann et al. 2022, Wohlleben et al. 2016). Furthermore, stronger cellular responses to SiO₂_15_Unmod compared to their surface-modified variants have also been observed in rat alveolar macrophage NR8383 (Wiemann et al. 2016) and epithelial RLE-6TN cells (Karkossa et al. 2019). In turn, SiO₂_40 caused a lower LDH release and did not alter metabolic activity compared to control RLE-6TN cells, most likely related to its largest size and lowest surface area, which is in agreement with the general consensus that particles with smaller size induce stronger biological effects than larger particles likely due to their specific surface area, which greatly increases their surface reactivity and cellular uptake (Oberdorster et al. 2005, Shang, Nienhaus, and Nienhaus 2014, Skuland et al. 2014). In this respect, and supporting our findings, Karkossa et al. (2019) reported that aSiO₂ NM surface area showed a positive correlation with mitochondrial dysfunction since an increased abundance for analytes connected to mitochondrial dysfunction was observed for the smaller building NM such as SiO₂_7, SiO₂_15_Unmod, SiO₂_15_Amino, and SiO₂_15_Phospho.

The genotoxic potential of aSiO₂ NM is far from being established. While some *in vitro* studies reported positive effects (Decan et al. 2016, Gonzalez et al. 2014, Maser et al. 2015, Mu et al.

2012), others showed no genotoxic effect from exposure to these NM (Guidi et al. 2015, Jin et al. 2007, Uboldi et al. 2012). DNA damage can be induced by direct interaction of the aSiO₂ NM with the DNA, or through indirect mechanisms such as the induction of oxidative stress (Kwon, Koedrith, and Seo 2014). Multi-omics analysis of RLE-6TN cells exposed to the same aSiO₂ NM variants tested herein revealed a significant enrichment of oxidative stress related pathways, mainly in cells exposed to SiO₂_40 (Karkossa et al. 2019, 2021), supporting the view that the DNA damaging ability of SiO₂_40 might be associated to the induction of oxidative stress in RLE-6TN cells. In agreement with this, previous *in vitro* studies have reported positive results for the genotoxic potential of aSiO₂ NM through indirect mechanisms in lung (Guichard et al. 2016, Maser et al. 2015, Mu et al. 2012). Nevertheless, differences in the genotoxic potential of aSiO₂ NM may also arise from their ability to enter the cell, distribute in the intracellular milieu and directly interact with the nucleus. Under serum-free conditions, as the ones adopted in this study, the physicochemical characteristic that most influences aSiO₂ NM ability to affect both plasma membrane and DNA integrity is the agglomerate size (Mu et al. 2012, Yazdimamaghani et al. 2019). In line with this view, Gonzalez et al. (2014) observed a hydrodynamic size-dependent increase of micronucleus (MN) frequency in A549 human lung carcinoma cells exposed to differently sized aSiO₂ NM, which was more pronounced in the absence of serum in the incubation medium. Moreover, Wiemann et al. (2021) also observed that the presence of serum mitigates the effects of precipitated and fumed aSiO₂ NM on alveolar macrophages by lowering their bioactivity and uptake in a particle specific manner.

Under our experimental conditions (in serum-free incubation medium), SiO₂_7_TMS2, SiO₂_7_TMS3, and SiO₂_40 did not exert a significant effect in the metabolic activity of rat alveolar epithelial cells. However, the remaining variants significantly decreased the metabolic activity of RLE-6TN cells and can be ranked for their cytotoxic potential as follows: SiO₂_15_Unmod > SiO₂_7 > SiO₂_15_Amino ~ SiO₂_15_Phospho. Interestingly, aSiO₂ NM variants with high cytotoxic potential such as SiO₂_7, SiO₂_15_Unmod and SiO₂_15_Amino were

negative for DNA damage, while SiO₂_40, the only aSiO₂ NM variant causing DNA damage did not induce cytotoxicity.

To deal with DNA damage, cells trigger DDR signaling cascades. To further explore the mechanisms involved in DNA damage and repair, we analyzed changes in cell cycle progression and γ -H2AX levels in response to exposure to selected aSiO₂ NM variants with high cyto- and genotoxic potential, i.e., SiO₂_7, SiO₂_15_Unmod, SiO₂_15_Amino, and SiO₂_40. Although no DNA damage was observed in cells exposed to SiO₂_7, SiO₂_15_Unmod and SiO₂_15_Amino, cell cycle arrest in S and G₂/M phases accompanied by a significant increase in histone H2AX phosphorylation was detected. Cell cycle arrest is an important mechanism during nanoparticle-induced DNA damage (Gonzalez et al. 2010) that provides time for repair mechanisms to occur prior progression to subsequent phases of the cell cycle (Uboldi et al. 2012), thus avoiding potential gene mutation (Schonn, Hennesen, and Dartsch 2010, Smith et al. 2010). At the S-phase checkpoint, the fidelity of DNA replication and the presence of unrepaired DNA damage are checked (Huang et al. 2008). In turn, G₂/M DNA damage checkpoint serves to prevent the cell from entering mitosis (M-phase) with genomic DNA damage (Gao et al. 2016). Cell cycle arrest at G₂/M and proliferation inhibition by SiO₂ NM exposure have previously been reported in human umbilical vein endothelial cells (HUVEC) exposed to SiO₂ NM, however DNA damage, as assessed by alkaline comet assay, was observed (Duan et al. 2013). The phosphorylation of H2AX plays a crucial role in the DDR by facilitating the recruitment of DNA repair proteins to sites of damaged chromatin (DSB) and activating checkpoint proteins that arrest cell cycle progression (Podhorecka, Skladanowski, and Bozko 2010). Furthermore, histone H2AX phosphorylation also occurs in response to replication arrest (Ward and Chen 2001) and initiation of DNA fragmentation during apoptosis (Rogakou et al. 2000). Thus, increased levels of γ -H2AX in RLE-6TN cells after exposure to the tested aSiO₂ NM (SiO₂_7, SiO₂_15_Unmod, and SiO₂_15_Amino), with no induction of DNA damage detected by the alkaline comet assay may be associated to the observed S- and G₂/M cell cycle arrest. Moreover, the possibility of other types of DNA damage, such as DNA interstrand crosslinks

(ICL), which can induce H2AX phosphorylation but may not be detected by the alkaline comet assay (Huang et al. 2004, Mogi and Oh 2006), or early apoptosis induction cannot be ruled out.

Whenever DNA injuries in the cells exceed cellular repair capacity, apoptosis may occur (Lu et al. 2006, Tanaka et al. 2006). At the same time, apoptosis is also associated with the occurrence of DNA breakage, however the relationship between apoptosis and the comet assay is complex since apoptotic cells may not appear as damaged cells in the comet assay, as the small oligonucleotides of late-stage apoptotic cells may disappear from the cellular area during electrophoresis (Azqueta et al. 2022). Herein, an increased number of cells in the sub-G1 population after exposure to the highest tested concentration of any of the three aSiO₂ variants, mostly in cells exposed to SiO₂_15_Amino, was observed. This finding is in agreement with Karkossa et al. (2021) that observed increased levels of metabolites such as proapoptotic Bax protein, sphingomyelins, and citric acid cycle enzymes [glutamate dehydrogenase 1 (Glud1) and fumarate hydratase (Fh)], which are associated to induction of apoptosis.

Genetic damage of another kind such as oxidative DNA damage, not detected in the standard alkaline comet assay, may occur, therefore, more studies are needed to further explore the underlying mechanisms through which these aSiO₂ NM induce genotoxicity and modulate DDR. Although SiO₂_40 induced DNA damage and increased γ H2AX levels of rat alveolar epithelial cells, mostly at G₀/G₁-phase, no alterations in the cell cycle progression were observed, suggesting the DNA damage detected in the alkaline comet assay correspond to DSB. DSB are one the most dangerous types of DNA damage which if left unrepaired lead to cell death (Podhorecka, Skladanowski, and Bozko 2010). In line with this, our results showed an increase of sub-G1 apoptotic cells in RLE-6TN cells exposed to 14 μ g/cm² of SiO₂_40, which was the concentration that caused the highest level of DNA damage in the rat alveolar cells.

With respect to the genotoxicity of aSiO₂ NM, there is a lack of correlation between *in vivo* and *in vitro* findings described in the literature, where most of the *in vitro* studies revealed positive genotoxic effects, contrasting with the absence of

significant genotoxic risk *in vivo* (Yazdimamaghani et al. 2019). However, evidence exists that *in vitro* studies can be predictive of *in vivo* genotoxicity. In this regard, Haase et al. (2017) showed that ZrO₂acrylate and SiO₂.amino NM were not genotoxic to human 3D bronchial EpiAirwayTM 3D cultures nor to rats following short-term inhalation (STIS). In this study, we showed a positive genotoxic effect for SiO₂_7 and SiO₂_40 in rat alveolar epithelial RLE-6TN cells, which is in agreement with a previous *in vivo* study from our group where oxidative DNA damage in the lung cells of rats intratracheally instilled with the same variants was detected, though the damage seemed repairable (Brandão et al. 2021). In addition, the low DNA damaging potential of SiO₂_15_Amino also agrees with previous observations *in vitro* in EpiAirwayTM cultures and *in vivo* in rats after short-term exposure (Haase et al. 2017). *In vitro* concentrations tested in this study matched *in vivo* calculated deposited doses, except for the highest tested dose, which may explain the absence of genotoxic potential of SiO₂_15_Unmod *in vivo* (Brandão et al. 2021) but a positive genotoxic potential *in vitro*. In addition, pyrogenic aSiO₂ NM (SiO₂_7 and SiO₂_40) caused more pronounced effects *in vivo* (alterations in lung DNA, protein integrity, and gene expression) compared to colloidal aSiO₂ NM (SiO₂_15_Unmod and SiO₂_15_Amino) as reported herein, demonstrating that the route of synthesis seems to play a role on aSiO₂ NM toxicity, which is in accordance with previous reports describing more pronounced effects caused by pyrogenic than precipitated aSiO₂ NM (Arts et al. 2007, Di Cristo et al. 2016, Karkossa et al. 2021).

Although the implemented ranking approach has some limitations, namely the low number of endpoints considered, we were able to successfully identify aSiO₂ NM variants that might require closer evaluation. In future studies, adding other genotoxicity endpoints, such as micronuclei formation, will be crucial to enhance the accuracy and the comprehensiveness of the ranking process.

5. Conclusion

Our study highlights the suitability and usefulness of a multiparametric approach to define aSiO₂ NM mechanism of action, and rank their hazard to pulmonary cells, with a focus on genotoxicity. Overall,

no major changes in the DNA integrity were detected in response to the aSiO₂ NM variants tested, though increases in H2AX phosphorylation were observed. Increasing the number of endpoints to assess would increase the robustness and reliability of the hazard ranking and provide a better understanding of their mode of action. The rat alveolar epithelial RLE-6TN cells seem to be a predictive model of aSiO₂ NM pulmonary toxicity *in vivo*. Surface modification with hydrophobic organosilanes, and in a lesser extent with phosphonate groups, seem to be an effective strategy to decrease the toxicity of aSiO₂ NM.

Acknowledgments

The authors would like to take this opportunity to thank all institutions involved for their support to this project.

Disclosure statement

The authors declare that the original work described is approved by all coauthors, has not been previously published and is not under consideration for publication elsewhere. In addition, the authors also declare that they have no conflicts of interest concerning this article.

Funding

This work was supported by the Portuguese Foundation for Science and Technology (FCT) through ERA-NET SIINN project NanoToxClass (SIINN/0001/2013). This work was also supported by the NanoBioBarriers project (POCI-01-0145-FEDER-031162), co-financed by the Operational Program for Competitiveness and Internationalization (POCI) through European Regional Development Funds (FEDER/FNR); and by the Spanish Ministry of Science and Innovation: MCIN/AEI/10.13039/501100011033 (Grant PID2020-114908GA-I00); and the Ministry of Education, Culture and Sport BEAGAL18/00142 to V. Valdiglesias. F. Brandão (SFRH/BD/101060/2014) and M.J. Bessa (SFRH/BD/12046/2016) are recipients of FCT PhD scholarships. The Doctoral Program in Biomedical Sciences of the ICBAS – University of Porto offered additional funds. S. Fraga thanks FCT for funding through program DL 57/2016 – Norma transitória (Ref. DL-57/INSA-06/2018). Thanks are also due to FCT/MCTES for the financial support to EPIUnit (UIDB/04750/2020) and ITR (LA/P/0064/2020).

ORCID

Fátima Brandão  <http://orcid.org/0000-0002-2933-8561>
 Carla Costa  <http://orcid.org/0000-0002-0027-8462>
 Maria João Bessa  <http://orcid.org/0000-0001-5357-6167>

Vanessa Valdiglesias  <http://orcid.org/0000-0002-5572-1089>

Andrea Haase  <http://orcid.org/0000-0002-5288-7876>

Sónia Fraga  <http://orcid.org/0000-0001-9386-2336>

João Paulo Teixeira  <http://orcid.org/0000-0001-8693-5250>

Data availability statement

The data sets used and/or analyzed during the current study are available from the corresponding authors on reasonable request.

References

- Ajdary, M., M. A. Moosavi, M. Rahmati, M. Falahati, M. Mahboubi, A. Mandegary, S. Jangjoo, R. Mohammadinejad, and R. S. Varma. 2018. "Health Concerns of Various Nanoparticles: A Review of Their *In Vitro* and *In Vivo* Toxicity." *Nanomaterials (Basel, Switzerland)* 8 (9): 8. <https://doi.org/10.3390/nano8090634>
- Arts, J. H., H. Muijser, E. Duistermaat, K. Junker, and C. F. Kuper. 2007. "Five-Day Inhalation Toxicity Study of Three Types of Synthetic Amorphous Silicas in Wistar Rats and Post-Exposure Evaluations for up to 3 Months." *Food and Chemical Toxicology* 45 (10): 1856–1867. <https://doi.org/10.1016/j.fct.2007.04.001>
- Azqueta, A., and A. R. Collins. 2013. "The Essential Comet Assay: A Comprehensive Guide to Measuring DNA Damage and Repair." *Archives of Toxicology* 87 (6): 949–968. <https://doi.org/10.1007/s00204-013-1070-0>
- Azqueta, A., and M. Dusinska. 2015. "The Use of the Comet Assay for the Evaluation of the Genotoxicity of Nanomaterials." *Frontiers in Genetics* 6: 239. <https://doi.org/10.3389/fgene.2015.00239>
- Azqueta, A., H. Stopper, B. Zegura, M. Dusinska, and P. Moller. 2022. "Do Cytotoxicity and Cell Death Cause False Positive Results in the *In Vitro* Comet Assay?" *Mutation Research. Genetic Toxicology and Environmental Mutagenesis* 881: 503520. <https://doi.org/10.1016/j.mrgentox.2022.503520>
- Bahl, A., B. Hellack, M. Balas, A. Dinischiotu, M. Wiemann, J. Brinkmann, A. Luch, B. Y. Renard, and A. Haase. 2019. "Recursive Feature Elimination in Random Forest Classification Supports Nanomaterial Grouping." *NanoImpact* 15: 100179. <https://doi.org/10.1016/j.impact.2019.100179>
- Bessa, M. J., C. Costa, J. Reinoso, C. Pereira, S. Fraga, J. Fernandez, M. A. Banares, and J. P. Teixeira. 2017. "Moving into Advanced Nanomaterials. Toxicity of Rutile TiO₂ Nanoparticles Immobilized in Nanokaolin Nanocomposites on HepG2 Cell Line." *Toxicology and Applied Pharmacology* 316: 114–122. <https://doi.org/10.1016/j.taap.2016.12.018>
- Brandão, F., C. Costa, M. J. Bessa, E. Dumortier, F. Debacq-Chainiaux, R. Hubaux, M. Salmon, et al. 2021. "Genotoxicity and Gene Expression in the Rat Lung Tissue following Instillation and Inhalation of Different Variants of Amorphous Silica Nanomaterials (aSiO₂ NM)." *Nanomaterials*

- (Basel, Switzerland) 11 (6): 11. <https://doi.org/10.3390/nano11061502>
- Chen, Z., Y. Wang, T. Ba, Y. Li, J. Pu, T. Chen, Y. Song, et al. 2014. "Genotoxic Evaluation of Titanium Dioxide Nanoparticles in Vivo and in Vitro." *Toxicology Letters* 226 (3): 314–319. <https://doi.org/10.1016/j.toxlet.2014.02.020>
- Clift, M. J. D., G. J. S. Jenkins, and S. H. Doak. 2020. "An Alternative Perspective towards Reducing the Risk of Engineered Nanomaterials to Human Health." *Small (Weinheim an Der Bergstrasse, Germany)* 16 (36): e2002002. <https://doi.org/10.1002/smll.202002002>
- Croissant, J. G., K. S. Butler, J. I. Zink, and C. J. Brinker. 2020. "Synthetic Amorphous Silica Nanoparticles: toxicity, Biomedical and Environmental Implications." *Nature Reviews Materials* 5 (12): 886–909. <https://doi.org/10.1038/s41578-020-0230-0>
- Decan, N., D. Wu, A. Williams, S. Bernatchez, M. Johnston, M. Hill, and S. Halappanavar. 2016. "Characterization of in Vitro Genotoxic, Cytotoxic and Transcriptomic Responses following Exposures to Amorphous Silica of Different Sizes." *Mutation Research. Genetic Toxicology and Environmental Mutagenesis* 796: 8–22. <https://doi.org/10.1016/j.mrgentox.2015.11.011>
- Di Cristo, L., D. Movia, M. G. Bianchi, M. Allegri, B. M. Mohamed, A. P. Bell, C. Moore, et al. 2016. "Proinflammatory Effects of Pyrogenic and Precipitated Amorphous Silica Nanoparticles in Innate Immunity Cells." *Toxicological Sciences: An Official Journal of the Society of Toxicology* 150 (1): 40–53. <https://doi.org/10.1093/toxsci/kfv258>
- Doak, S. H., and M. Dusinska. 2017. "NanoGenotoxicology: Present and the Future." *Mutagenesis* 32 (1): 1–4. <https://doi.org/10.1093/mutage/gew066>
- Duan, J., Y. Yu, Y. Li, Y. Yu, Y. Li, X. Zhou, P. Huang, and Z. Sun. 2013. "Toxic Effect of Silica Nanoparticles on Endothelial Cells through DNA Damage Response via Chk1-Dependent G2/M Checkpoint." *PLoS One* 8 (4): e62087. <https://doi.org/10.1371/journal.pone.0062087>
- Dusinska, M., E. Mariussen, E. Rundén-Pran, A. M. Hudcová, E. Elje, A. Kazimirova, N. El Yamani, N. Dommershausen, J. Tharmann, and D. Fieblinger. 2019. "In Vitro Approaches for Assessing the Genotoxicity of Nanomaterials." *Nanotoxicity*, 83–122. Berlin, Germany: Springer.
- El Yamani, N., A. R. Collins, E. Runden-Pran, L. M. Fjellsbo, S. Shaposhnikov, S. Zienolddiny, and M. Dusinska. 2017. "In Vitro Genotoxicity Testing of Four Reference Metal Nanomaterials, Titanium Dioxide, Zinc Oxide, Cerium Oxide and Silver: Towards Reliable Hazard Assessment." *Mutagenesis* 32 (1): 117–126. <https://doi.org/10.1093/mutage/gew060>
- Gao, F., N. Ma, H. Zhou, Q. Wang, H. Zhang, P. Wang, H. Hou, H. Wen, and L. Li. 2016. "Zinc Oxide Nanoparticles-Induced Epigenetic Change and G2/M Arrest Are Associated with Apoptosis in Human Epidermal Keratinocytes." *International Journal of Nanomedicine* 11: 3859–3874. <https://doi.org/10.2147/IJN.S107021>
- Gonzalez, L., M. Lukamowicz-Rajska, L. C. Thomassen, C. E. Kirschhock, L. Leyns, D. Lison, J. A. Martens, A. Elhajouji, and M. Kirsch-Volders. 2014. "Co-Assessment of Cell Cycle and Micronucleus Frequencies Demonstrates the Influence of Serum on the in Vitro Genotoxic Response to Amorphous Monodisperse Silica Nanoparticles of Varying Sizes." *Nanotoxicology* 8 (8): 876–884. <https://doi.org/10.3109/17435390.2013.842266>
- Gonzalez, L., L. C. Thomassen, G. Plas, V. Rabolli, D. Napierska, I. Decordier, M. Roelants, et al. 2010. "Exploring the Aneugenic and Clastogenic Potential in the Nanosize Range: A549 Human Lung Carcinoma Cells and Amorphous Monodisperse Silica Nanoparticles as Models." *Nanotoxicology* 4 (4): 382–395. <https://doi.org/10.3109/17435390.2010.501913>
- Großgarten, M., M. Holzlechner, A. Vennemann, A. Balbekova, K. Wieland, M. Sperling, B. Lendl, M. Marchetti-Deschmann, U. Karst, and M. Wiemann. 2018. "Phosphonate Coating of SiO₂ Nanoparticles Abrogates Inflammatory Effects and Local Changes of the Lipid Composition in the Rat Lung: A Complementary Bioimaging Study." *Particle and Fibre Toxicology* 15 (1): 31. <https://doi.org/10.1186/s12989-018-0267-z>
- Guadagnini, R., B. Halamoda Kenzaoui, L. Walker, G. Pojana, Z. Magdolenova, D. Bilanicova, M. Saunders, et al. 2015. "Toxicity Screenings of Nanomaterials: challenges Due to Interference with Assay Processes and Components of Classic in Vitro Tests." *Nanotoxicology* 9 (1): 13–24. <https://doi.org/10.3109/17435390.2013.829590>
- Guichard, Y., C. Fontana, E. Chaviner, F. Terzetti, L. Gate, S. Binet, and C. Darne. 2016. "Cytotoxic and Genotoxic Evaluation of Different Synthetic Amorphous Silica Nanomaterials in the V79 Cell Line." *Toxicology and Industrial Health* 32 (9): 1639–1650. <https://doi.org/10.1177/0748233715572562>
- Guidi, P., M. Nigro, M. Bernardeschi, P. Lucchesi, V. Scarcelli, and G. Frenzilli. 2015. "Does the Crystal Habit Modulate the Genotoxic Potential of Silica Particles? A Cytogenetic Evaluation in Human and Murine Cell Lines." *Mutation Research. Genetic Toxicology and Environmental Mutagenesis* 792: 46–52. <https://doi.org/10.1016/j.mrgentox.2015.07.005>
- Gurcan, C., H. Taheri, A. Bianco, L. G. Delogu, and A. Yilmazer. 2020. "A Closer Look at the Genotoxicity of Graphene Based Materials." *Journal of Physics: Materials* 3 (1): 014007. <https://doi.org/10.1088/2515-7639/ab5844>
- Haase, A., N. Dommershausen, M. Schulz, R. Landsiedel, P. Reichardt, B. C. Krause, J. Tentschert, and A. Luch. 2017. "Genotoxicity Testing of Different Surface-Functionalized SiO₂, ZrO₂ and Silver Nanomaterials in 3D Human Bronchial Models." *Archives of Toxicology* 91 (12): 3991–4007. <https://doi.org/10.1007/s00204-017-2015-9>
- Halamoda-Kenzaoui, B., M. Ceridono, P. Colpo, A. Valsesia, P. Urbán, I. Ojea-Jiménez, S. Gioria, D. Gilliland, F. Rossi, and A. Kinsner-Ovaskainen. 2015. "Dispersion Behaviour of Silica Nanoparticles in Biological Media and Its Influence

- on Cellular Uptake." *PLoS One* 10 (10): e0141593. <https://doi.org/10.1371/journal.pone.0141593>
- Hiemstra, P. S., G. Grootaers, A. M. van der Does, C. A. M. Krul, and I. M. Kooter. 2018. "Human Lung Epithelial Cell Cultures for Analysis of Inhaled Toxicants: Lessons Learned and Future Directions." *Toxicology in Vitro: An International Journal Published in Association with BIBRA* 47: 137–146. <https://doi.org/10.1016/j.tiv.2017.11.005>
- Huang, M., Z.-H. Miao, H. Zhu, Y.-J. Cai, W. Lu, and J. Ding. 2008. "Chk1 and Chk2 Are Differentially Involved in Homologous Recombination Repair and Cell Cycle Arrest in Response to DNA Double-Strand Breaks Induced by Camptothecins." *Molecular Cancer Therapeutics* 7 (6): 1440–1449. <https://doi.org/10.1158/1535-7163.MCT-07-2116>
- Huang, X., and Z. Darzynkiewicz. 2006. *Cytometric Assessment of Histone H2AX Phosphorylation. DNA Repair Protocols*, 73–80. Berlin, Germany: Springer.
- Huang, X., M. Okafuji, F. Traganos, E. Luther, E. Holden, and Z. Darzynkiewicz. 2004. "Assessment of Histone H2AX Phosphorylation Induced by DNA Topoisomerase I and II Inhibitors Topotecan and Mitoxantrone and by the DNA Cross-Linking Agent Cisplatin." *Cytometry. Part A: The Journal of the International Society for Analytical Cytology* 58 (2): 99–110. <https://doi.org/10.1002/cyto.a.20018>
- Jiao, Z., J. Chang, J. Li, D. Nie, H. Cui, and D. Guo. 2017. "Sulforaphane Increases Nrf2 Expression and Protects Alveolar Epithelial Cells against Injury Caused by Cigarette Smoke Extract." *Molecular Medicine Reports* 16 (2): 1241–1247. <https://doi.org/10.3892/mmr.2017.6700>
- Jin, Y., S. Kannan, M. Wu, and J. X. Zhao. 2007. "Toxicity of Luminescent Silica Nanoparticles to Living Cells." *Chemical Research in Toxicology* 20 (8): 1126–1133. <https://doi.org/10.1021/tx7001959>
- Karkossa, I., A. Bannuscher, B. Hellack, A. Bahl, S. Buhs, P. Nollau, A. Luch, K. Schubert, M. von Bergen, and A. Haase. 2019. "An in-Depth Multi-Omics Analysis in RLE-6TN Rat Alveolar Epithelial Cells Allows for Nanomaterial Categorization." *Particle and Fibre Toxicology* 16 (1): 38. <https://doi.org/10.1186/s12989-019-0321-5>
- Karkossa, I., A. Bannuscher, B. Hellack, W. Wohlleben, J. Laloy, M. S. Stan, A. Dinischiotu, et al. 2021. "Nanomaterials Induce Different Levels of Oxidative Stress, Depending on the Used Model System: Comparison of in Vitro and in Vivo Effects." *The Science of the Total Environment* 801: 149538. <https://doi.org/10.1016/j.scitotenv.2021.149538>
- Kasper, J. Y., L. Feiden, M. I. Hermanns, C. Bantz, M. Maskos, R. E. Unger, and C. J. Kirkpatrick. 2015. "Pulmonary Surfactant Augments Cytotoxicity of Silica Nanoparticles: Studies on an in Vitro Air–Blood Barrier Model." *Beilstein Journal of Nanotechnology* 6: 517–528. <https://doi.org/10.3762/bjnano.6.54>
- Kroll, A., C. Dierker, C. Rommel, D. Hahn, W. Wohlleben, C. Schulze-Isfort, C. Göbber, M. Voetz, F. Hardinghaus, and J. Schneckeburger. 2011. "Cytotoxicity Screening of 23 Engineered Nanomaterials Using a Test Matrix of Ten Cell Lines and Three Different Assays." *Particle and Fibre Toxicology* 8 (1): 9. <https://doi.org/10.1186/1743-8977-8-9>
- Kroll, A., M. H. Pillukat, D. Hahn, and J. Schneckeburger. 2012. "Interference of Engineered Nanoparticles with in Vitro Toxicity Assays." *Archives of Toxicology* 86 (7): 1123–1136. <https://doi.org/10.1007/s00204-012-0837-z>
- Kryston, T. B., A. B. Georgiev, P. Pissis, and A. G. Georgakilas. 2011. "Role of Oxidative Stress and DNA Damage in Human Carcinogenesis." *Mutation Research* 711 (1–2): 193–201. <https://doi.org/10.1016/j.mrfmmm.2010.12.016>
- Kwon, J. Y., P. Koedrith, and Y. R. Seo. 2014. "Current Investigations into the Genotoxicity of Zinc Oxide and Silica Nanoparticles in Mammalian Models in Vitro and in Vivo: Carcinogenic/Genotoxic Potential, Relevant Mechanisms and Biomarkers, Artifacts, and Limitations." *International Journal of Nanomedicine* 9 (2): 271–286. <https://doi.org/10.2147/IJN.S57918>
- Landsiedel, R., N. Honarvar, S. B. Seiffert, B. Oesch, and F. Oesch. 2022. "Genotoxicity Testing of Nanomaterials." *Wiley Interdisciplinary Reviews. Nanomedicine and Nanobiotechnology* 14 (6): e1833. <https://doi.org/10.1002/wnan.1833>
- Lankoff, A., M. Arabski, A. Wegierek-Ciuk, M. Kruszewski, H. Lisowska, A. Banasik-Nowak, K. Rozga-Wijas, M. Wojewodzka, and S. Slomkowski. 2013. "Effect of Surface Modification of Silica Nanoparticles on Toxicity and Cellular Uptake by Human Peripheral Blood Lymphocytes in Vitro." *Nanotoxicology* 7 (3): 235–250. <https://doi.org/10.3109/17435390.2011.649796>
- Lu, C., F. Zhu, Y. Y. Cho, F. Tang, T. Zykova, W. Y. Ma, A. M. Bode, and Z. Dong. 2006. "Cell Apoptosis: Requirement of H2AX in DNA Ladder Formation, but Not for the Activation of Caspase-3." *Molecular Cell* 23 (1): 121–132. <https://doi.org/10.1016/j.molcel.2006.05.023>
- Mazzioli, V., J. A. Aguilar-Pimentel, I. Weichenmeier, G. Luxenhofer, M. Wiemann, R. Landsiedel, W. Wohlleben, et al. 2014. "Surface Modifications of Silica Nanoparticles Are Crucial for Their Inert versus Proinflammatory and Immunomodulatory Properties." *International Journal of Nanomedicine* 9: 2815–2832. <https://doi.org/10.2147/IJN.S57396>
- Maser, E., M. Schulz, U. G. Sauer, M. Wiemann, L. Ma-Hock, W. Wohlleben, A. Hartwig, and R. Landsiedel. 2015. "In Vitro and in Vivo Genotoxicity Investigations of Differently Sized Amorphous SiO₂ Nanomaterials." *Mutation Research. Genetic Toxicology and Environmental Mutagenesis* 794: 57–74. <https://doi.org/10.1016/j.mrgento.2015.10.005>
- Mogi, S., and D. H. Oh. 2006. "γ-H2AX Formation in Response to Interstrand Crosslinks Requires XPF in Human Cells." *DNA Repair* 5 (6): 731–740. <https://doi.org/10.1016/j.dnarep.2006.03.009>
- Moller, P., A. Azqueta, E. Boutet-Robinet, G. Koppen, S. Bonassi, M. Milic, G. Gajski, et al. 2020. "Minimum Information for Reporting on the Comet Assay (MIRCA): Recommendations for Describing Comet Assay Procedures

- and Results." *Nature Protocols* 15 (12): 3817–3826. <https://doi.org/10.1038/s41596-020-0398-1>
- Mu, Q., N. S. Hondow, L. Krzemiński, A. P. Brown, L. J. C. Jeuken, and M. N. Routledge. 2012. "Mechanism of Cellular Uptake of Genotoxic Silica Nanoparticles." *Particle and Fibre Toxicology* 9 (1): 29. <https://doi.org/10.1186/1743-8977-9-29>
- NanoToxClass. 2017. NanoToxClass Standard Operation Procedure - Preparation of Nanoparticle Suspensions by Cup Horn Sonication. https://www.nanopartikel.info/NanoToxClassSOP_Dispersion.
- Nayl, A. A., A. I. Abd-Elhamid, A. A. Aly, and S. Brase. 2022. "Recent Progress in the Applications of Silica-Based Nanoparticles." *RSC Advances* 12 (22): 13706–13726. <https://doi.org/10.1039/d2ra01587k>
- Nikolova, T., F. Marini, and B. Kaina. 2017. "Genotoxicity Testing: Comparison of the gammaH2AX Focus Assay with the Alkaline and Neutral Comet Assays." *Mutation Research. Genetic Toxicology and Environmental Mutagenesis* 822: 10–18. <https://doi.org/10.1016/j.mrgentox.2017.07.004>
- Oberdorster, G., A. Maynard, K. Donaldson, V. Castranova, J. Fitzpatrick, K. Ausman, J. Carter, et al. 2005. "Principles for Characterizing the Potential Human Health Effects from Exposure to Nanomaterials: elements of a Screening Strategy." *Particle and Fibre Toxicology* 2 (1): 8. <https://doi.org/10.1186/1743-8977-2-8>
- Oda, K., R. Yumoto, J. Nagai, H. Katayama, and M. Takano. 2011. "Mechanism Underlying Insulin Uptake in Alveolar Epithelial Cell Line RLE-6TN." *European Journal of Pharmacology* 672 (1–3): 62–69. <https://doi.org/10.1016/j.ejphar.2011.10.003>
- OECD. 2014. "Genotoxicity of Manufactured Nanomaterials: Report of the Oecd Expert." *Series on the Safety of Manufactured Nanomaterials*. Paris, France: OECD.
- OECD. 2016a. *Test No. 473: In Vitro Mammalian Chromosomal Aberration Test*. Paris, France: OECD.
- OECD. 2016b. *Test No. 476: In Vitro Mammalian Cell Gene Mutation Tests Using the Hprt and Xprt Genes*. Paris, France: OECD.
- OECD. 2016c. *Test No. 487: In Vitro Mammalian Cell Micronucleus Test*. Paris, France: OECD.
- OECD. 2016d. *Test No. 490: In Vitro Mammalian Cell Gene Mutation Tests Using the Thymidine Kinase Gene*. Paris, France: OECD.
- Pauluhn, J. 2009. "Comparative Pulmonary Response to Inhaled Nanostructures: considerations on Test Design and Endpoints." *Inhalation Toxicology* 21 (1): 40–54. <https://doi.org/10.1080/08958370902962291>
- Pietroiusti, A., H. Stockmann-Juvala, F. Lucaroni, and K. Savolainen. 2018. "Nanomaterial Exposure, Toxicity, and Impact on Human Health." *Wiley Interdisciplinary Reviews. Nanomedicine and Nanobiotechnology* 10 (5): e1513. <https://doi.org/10.1002/wnan.1513>
- Podhorecka, M., A. Skladanowski, and P. Bozko. 2010. "H2AX Phosphorylation: Its Role in DNA Damage Response and Cancer Therapy." *Journal of Nucleic Acids* 2010: 1–9. <https://doi.org/10.4061/2010/920161>
- Rogakou, E. P., W. Nieves-Neira, C. Boon, Y. Pommier, and W. M. Bonner. 2000. "Initiation of DNA Fragmentation during Apoptosis Induces Phosphorylation of H2AX Histone at Serine 139." *The Journal of Biological Chemistry* 275 (13): 9390–9395. <https://doi.org/10.1074/jbc.275.13.9390>
- Rogakou, E. P., D. R. Pilch, A. H. Orr, V. S. Ivanova, and W. M. Bonner. 1998. "DNA Double-Stranded Breaks Induce Histone H2AX Phosphorylation on Serine 139." *The Journal of Biological Chemistry* 273 (10): 5858–5868. <https://doi.org/10.1074/jbc.273.10.5858>
- Rosário, F., M. J. Bessa, F. Brandão, C. Costa, C. B. Lopes, A. C. Estrada, D. S. Tavares, J. P. Teixeira, and A. T. Reis. 2020. "Unravelling the Potential Cytotoxic Effects of Metal Oxide Nanoparticles and Metal (Loid) Mixtures on A549 Human Cell Line." *Nanomaterials* 10 (3): 447. <https://doi.org/10.3390/nano10030447>
- Scarpato, R., S. Castagna, R. Aliotta, A. Azzara, F. Ghetti, E. Filomeni, C. Giovannini, et al. 2013. "Kinetics of Nuclear Phosphorylation (gamma-H2AX) in Human Lymphocytes Treated in Vitro with UVB, Bleomycin and Mitomycin C." *Mutagenesis* 28 (4): 465–473. <https://doi.org/10.1093/mutage/get024>
- Schonn, I., J. Hennesen, and D. C. Dartsch. 2010. "Cellular Responses to Etoposide: Cell Death despite Cell Cycle Arrest and Repair of DNA Damage." *Apoptosis: An International Journal on Programmed Cell Death* 15 (2): 162–172. <https://doi.org/10.1007/s10495-009-0440-9>
- Shang, L., K. Nienhaus, and G. U. Nienhaus. 2014. "Engineered Nanoparticles Interacting with Cells: Size Matters." *Journal of Nanobiotechnology* 12 (1): 5. <https://doi.org/10.1186/1477-3155-12-5>
- Shatkin, J. A. 2008. *Introduction: Assessing Nanotechnology Health and Environmental Risks*. Nanotechnology, 21–40. Boca Raton, FL: CRC Press.
- Skuland, T., J. Øvrevik, M. Låg, and M. Refsnes. 2014. "Role of Size and Surface Area for Pro-Inflammatory Responses to Silica Nanoparticles in Epithelial Lung Cells: Importance of Exposure Conditions." *Toxicology in Vitro: An International Journal Published in Association with BIBRA* 28 (2): 146–155. <https://doi.org/10.1016/j.tiv.2013.10.018>
- Smith, J., L. M. Tho, N. Xu, and D. A. Gillespie. 2010. "The ATM-Chk2 and ATR-Chk1 Pathways in DNA Damage Signaling and Cancer." *Advances in Cancer Research* 108: 73–112. <https://doi.org/10.1016/B978-0-12-380888-2.00003-0>
- Stone, V., M. R. Miller, M. J. D. Clift, A. Elder, N. L. Mills, P. Moller, R. P. F. Schins, et al. 2017. "Nanomaterials versus Ambient Ultrafine Particles: An Opportunity to Exchange Toxicology Knowledge." *Environmental Health Perspectives* 125 (10): 106002. <https://doi.org/10.1289/EHP424>
- Swedish Chemicals Agency. 2016. Report 13/16 *Nanomaterials and Genotoxicity - a Literature Review*, ISSN 0284-1185. Article number: 361 218.
- Tanaka, T., A. Kurose, X. Huang, W. Dai, and Z. Darzynkiewicz. 2006. "ATM Activation and Histone H2AX Phosphorylation as Indicators of DNA Damage by DNA Topoisomerase I Inhibitor Topotecan and during

- Apoptosis." *Cell Proliferation* 39 (1): 49–60. <https://doi.org/10.1111/j.1365-2184.2006.00364.x>
- Tomilin, N., L. Solovjeva, M. Svetlova, N. Pleskach, I. Zalenskaya, P. Yau, and E. Bradbury. 2001. "Visualization of Focal Nuclear Sites of DNA Repair Synthesis Induced by Bleomycin in Human Cells." *Radiation Research* 156 (4): 347–354. [https://doi.org/10.1667/0033-7587\(2001\)156\[0347:VOFNSO2.0.CO;2\]](https://doi.org/10.1667/0033-7587(2001)156[0347:VOFNSO2.0.CO;2])
- Tsuji, J. S., A. D. Maynard, P. C. Howard, J. T. James, C. W. Lam, D. B. Warheit, and A. B. Santamaria. 2006. "Research Strategies for Safety Evaluation of Nanomaterials, Part IV: risk Assessment of Nanoparticles." *Toxicological Sciences: An Official Journal of the Society of Toxicology* 89 (1): 42–50. <https://doi.org/10.1093/toxsci/kfi339>
- Uboldi, C., G. Giudetti, F. Broggi, D. Gilliland, J. Ponti, and F. Rossi. 2012. "Amorphous Silica Nanoparticles Do Not Induce Cytotoxicity, Cell Transformation or Genotoxicity in Balb/3T3 Mouse Fibroblasts." *Mutation Research* 745 (1–2): 11–20. <https://doi.org/10.1016/j.mrgentox.2011.10.010>
- Valdiglesias, V., S. Giunta, M. Fenech, M. Neri, and S. Bonassi. 2013. "γH2AX as a Marker of DNA Double Strand Breaks and Genomic Instability in Human Population Studies." *Mutation Research* 753 (1): 24–40. <https://doi.org/10.1016/j.mrrev.2013.02.001>
- Valdiglesias, V., B. Laffon, E. Pásaro, and J. Méndez. 2011. "Evaluation of Okadaic Acid-Induced Genotoxicity in Human Cells Using the Micronucleus Test and γH2AX Analysis." *Journal of Toxicology and Environmental Health. Part A* 74 (15–16): 980–992. <https://doi.org/10.1080/15287394.2011.582026>
- Vance, M. E., T. Kuiken, E. P. Vejerano, S. P. McGinnis, M. F. Hochella, Jr., D. Rejeski, and M. S. Hull. 2015. "Nanotechnology in the Real World: Redeveloping the Nanomaterial Consumer Products Inventory." *Beilstein Journal of Nanotechnology* 6: 1769–1780. <https://doi.org/10.3762/bjnano.6.181>
- Wan, R., Y. Mo, R. Tong, M. Gao, and Q. Zhang. 2019. "Determination of Phosphorylated Histone H2AX in Nanoparticle-Induced Genotoxic Studies." *Methods in Molecular Biology* 1894: 145–159. https://doi.org/10.1007/978-1-4939-8916-4_9
- Ward, I. M., and J. Chen. 2001. "Histone H2AX is Phosphorylated in an ATR-Dependent Manner in Response to Replicational Stress." *The Journal of Biological Chemistry* 276 (51): 47759–47762. <https://doi.org/10.1074/jbc.C100569200>
- Wiemann, M., A. Vennemann, U. G. Sauer, K. Wiench, L. Ma-Hock, and R. Landsiedel. 2016. "An in Vitro Alveolar Macrophage Assay for Predicting the Short-Term Inhalation Toxicity of Nanomaterials." *Journal of Nanobiotechnology* 14 (1): 16. <https://doi.org/10.1186/s12951-016-0164-2>
- Wiemann, M., A. Vennemann, T. B. Schuster, J. Nolde, and N. Krueger. 2022. "Surface Treatment with Hydrophobic Coating Reagents (Organosilanes) Strongly Reduces the Bioactivity of Synthetic Amorphous Silica in Vitro." *Frontiers in Public Health* 10: 902799. <https://doi.org/10.3389/fpubh.2022.902799>
- Wiemann, M., A. Vennemann, C. Venzago, G. G. Lindner, T. B. Schuster, and N. Krueger. 2021. "Serum Lowers Bioactivity and Uptake of Synthetic Amorphous Silica by Alveolar Macrophages in a Particle Specific Manner." *Nanomaterials* 11 (3): 628. <https://doi.org/10.3390/nano11030628>
- Wohlleben, W., M. D. Driessen, S. Raesch, U. F. Schaefer, C. Schulze, B. Vacano, A. Vennemann, et al. 2016. "Influence of Agglomeration and Specific Lung Lining Lipid/Protein Interaction on Short-Term Inhalation Toxicity." *Nanotoxicology* 10 (7): 970–980. <https://doi.org/10.3109/17435390.2016.1155671>
- Yazdimamaghani, M., P. J. Moos, M. A. Dobrovolskaia, and H. Ghandehari. 2019. "Genotoxicity of Amorphous Silica Nanoparticles: Status and Prospects." *Nanomedicine: Nanotechnology, Biology, and Medicine* 16: 106–125. <https://doi.org/10.1016/j.nano.2018.11.013>
- Yoshida, T., Y. Yoshioka, K. Matsuyama, Y. Nakazato, S. Tochigi, T. Hirai, S. Kondoh, et al. 2012. "Surface Modification of Amorphous Nanosilica Particles Suppresses Nanosilica-Induced Cytotoxicity, ROS Generation, and DNA Damage in Various Mammalian Cells." *Biochemical and Biophysical Research Communications* 427 (4): 748–752. <https://doi.org/10.1016/j.bbrc.2012.09.132>
- Zhang, H., D. R. Dunphy, X. Jiang, H. Meng, B. Sun, D. Tarn, M. Xue, et al. 2012. "Processing Pathway Dependence of Amorphous Silica Nanoparticle Toxicity: Colloidal vs Pyrolytic." *Journal of the American Chemical Society* 134 (38): 15790–15804. <https://doi.org/10.1021/ja304907c>